NJC

ROYAL SOCIETY OF CHEMISTRY

PAPER

View Article Online
View Journal

Cite this: DOI: 10.1039/d0nj05327a

Bis-maltol-polyamine family: structural modifications at strategic positions. Synthesis, coordination and antineoplastic activity of two new ligands†

Luca Giorgi, [a] Gianluca Ambrosi, [a] Daniele Paderni, [a] Luca Conti, [b] Stefano Amatori, [c] Francesca Romagnoli, [a] Patrizia Rossi, [d] Mauro Formica, [a] Eleonora Macedi, *[a] Claudia Giorgi, [b] Paola Paoli, [d] Mirco Fanelli [c] and Vieri Fusi *[a]

Received 30th October 2020,
Accepted 30th December 2020

DOI: 10.1039/d0nj05327a

rsc.li/njc

Two new maltol-based ligands are presented, **L1** (*N*,*N*′-bis((3-hydroxy-6-methyl-4-pyron-2-yl)methyl)-*N*,*N*′-dimethylethylenediamine) and **L2** (*N*,*N*′-bis((3-hydroxy-6-hydroxymethyl-4-pyron-2-yl)methyl)-*N*,*N*′-dimethylethylenediamine). They were strategically designed by inserting a methyl or hydroxymethyl function at C6, to study the previously hypothesized involvement of that ring position in the anticancer properties and the peculiar metal coordination ability in aqueous solution already shown by this family of ligands. Solid state and solution studies revealed differences neither in the molecular conformation or crystal packing nor in the acid–base behavior compared with the precursor Malten. The introduced substituent groups seem to affect instead both the degradation time (*ca.* 4–5 h for **L1** and **L2** *vs.* 10 h for Malten) and the binding properties towards Cu(II), Zn(II) and Co(II), log *K* values being the highest for **L1** within the series of the diamino-bis-maltol ligands. The introduction of $-CH_2OH$ at C6 is sufficient to impair the biological activity of the compound and is coherent with the hypothesized mechanism of action.

1. Introduction

Worldwide, cancer is still one of the major leading causes of death. Much progress has been made against it over the last century, nevertheless numerous challenges still prevent the possibility of providing the best outcome for patients. A WHO report claims that annual cancer cases are expected to rise from 14 million in 2012 to 26 million within the next 2 decades.[1]

Thus, despite the recent advances, much work remains. Effort must be made to identify good molecular targets (playing key roles in cancer cell growth and survival) and to design and develop drugs able to bind to them, to develop treatments that are more specific and effective and less toxic (targeted therapies, immunotherapies and cancer vaccines), to overcome drug resistance and to improve conventional treatments such as chemotherapy, radiation therapy and surgery.

Finding new antineoplastic drugs with reduced toxicity and higher selectivity is therefore a major therapeutic goal. Natural products are useful both as biological tools as well as therapeutic agents and continue to be inspiring model compounds in medicinal chemistry.

In our previous studies a class of molecules has been developed, constituted of a variable polyamine framework decorated with the naturally occurring substance maltol (3-hydroxy-2-methyl-4-pyrone, Fig. 1) as a binding unit. These molecules combine the known acid–base properties, biocompatibility,[2–6] and antioxidant and coordination properties[7] of maltol with the antitumor features of linear and macrocyclic polyamines.

Such a combination could prove very fruitful indeed, since on one hand, maltol possesses ROS scavenger and antioxidant properties that provide the molecule with antineoplastic,[8] neuroprotective[9,10] and anti-apoptotic activities;[11] in addition, both maltol-derived organometallic complexes[12,13] and maltol-containing ligands have potential antitumor activity.[14]

On the other hand, rapidly proliferating cells (including cancer cells) require a higher amount of polyamines than normal cells,

[a] *Dipartimento di Scienze Pure e Applicate, Università degli Studi di Urbino "Carlo Bo", via della Stazione 4, I-61029 Urbino, Italy. E-mail: eleonora.macedi@uniurb.it, vieri.fusi@uniurb.it*
[b] *Department of Chemistry "Ugo Schiff", University of Florence, via della Lastruccia 3-13, 50019 Sesto Fiorentino, Italy*
[c] *Department of Biomolecular Sciences, Molecular Pathology Laboratory "PaoLa" University of Urbino "Carlo Bo", via Arco d' Augusto 2, 61032 Fano, Italy*
[d] *Department of Industrial Engineering, University of Florence, via S. Marta 3, 50139 Florence, Italy*

† Electronic supplementary information (ESI) available: Crystallographic data are provided in PDF format. CCDC 2040416. For ESI and crystallographic data in CIF or other electronic format see DOI: 10.1039/d0nj05327a

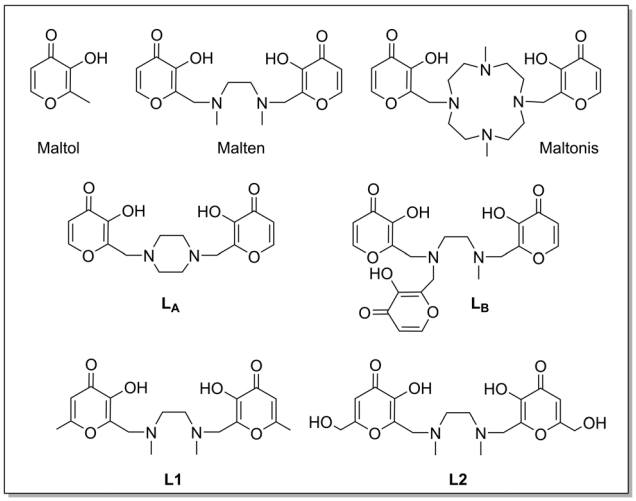

Fig. 1 Compounds Maltol, Malten, Maltonis, $\mathbf{L_A}$, $\mathbf{L_B}$, **L1** and **L2**.

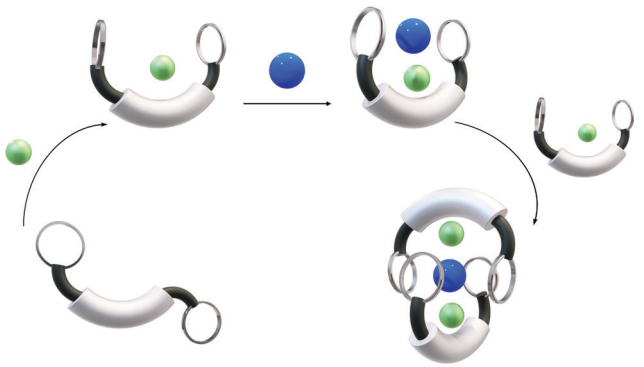

Fig. 2 Coordination scheme of maltol-based ligands towards metal cations. Green sphere: transition metal ion; blue sphere: alkaline, alkaline-earth or rare earth metal ion.

thus polyamine-depleting agents might be used in cancer treatment.[15] Studies showed that synthetic polyamine analogues, structurally similar to the biogenic polyamines without being able to functionally substitute them,[16,17] are able to interfere with the polyamine biosynthesis and to cause polyamine depletion.[18,19] Due to these features and to the relatively non-toxic response in normal tissues, polyamine analogues are presently being tested in human cancer patients as potential new chemotherapeutic agents, both individually and collectively as well as in combination with other anticancer drugs or traditional chemotherapeutics.[20–22]

Two of the synthesized maltol-based polyamine ligands, showing two [(3-hydroxy-4-pyron-2-yl)methyl]amine units separated by either a linear (*N*,*N*′-bis((3-hydroxy-4-pyron-2-yl)methyl)-*N*,*N*′-dimethylethylenediamine, Malten, Fig. 1) or cyclic (4,10-bis[(3-hydroxy-4-pyron-2-yl)methyl]-1,7-dimethyl-1,4,7,10-tetraazacyclododecane, Maltonis, Fig. 1) aliphatic amine spacer, exhibited anti-neoplastic activity *in vitro*[23] and *in vivo*.[24]

Studies on Malten and Maltonis showed an antiproliferative effect due to complex structural alterations of genomic DNA possibly induced by DNA intermolecular crosslinking. The genomic alterations lead to a dose-dependent reduction in cell survival and activation of both cell cycle arrest and programmed cell death (apoptosis) as a function of the modulation in the expression of genes having key roles in DNA-damage response, cell cycle progression and apoptosis.[23,24] Both ligands are able to favor the covalent binding between DNA and proteins, suggesting an interference with the chromatin structure as a possible molecular mechanism of action.[23,24] Finally, the simultaneous presence of two amino-spaced maltol units seems to be crucial for the biological activity of the molecules.

Malten and Maltonis also showed peculiar binding properties towards metal ions in aqueous solution (Fig. 2). They are able to coordinate a transition metal cation (green sphere in Fig. 2) in an "inner" location (binding site provided by the polyamine scaffold and hydroxyl groups of maltol moieties), preorganizing the molecule, otherwise arranged in a stretched conformation,[23d] in a way that maltol units converge to form a second binding area featuring a harder nature [binding site provided by hydroxyl (bridging donor groups) and carbonyl groups of maltol moieties] and able to lodge metal cations generally recognized as difficult to bind in water, such as those of the alkaline, alkaline-earth and rare earth series (blue sphere in Fig. 2). Mostly, heterotrinuclear dimers form, where two transition metal complexes stabilize one hard metal cation[25] (Fig. 2), but mononuclear and heterodinuclear monomers as discrete entities[26] or metal coordination polymers[25b,27] as well as homo-[26] and heterotetranuclear dimers[25b,28] were also obtained.

Following principles of drug discovery, according to which the research of a new pharmacologically active molecule begins from a lead compound that shows biological activity but may be improved, we have been modifying the structure of Malten providing it with strategic features that can eventually help us to both gain a better comprehension of the mechanism of action as well as modify the biological activity of the compound.

To this purpose, we have recently expanded the maltol-based ligand family by synthesizing two Malten derivatives, *N*,*N*′-bis((3-hydroxy-4-pyron-2-yl)methyl)-1,4-piperazine ($\mathbf{L_A}$ in Fig. 1) and *N*,*N*′,*N*′-tris((3-hydroxy-4-pyron-2-yl)methyl)-*N*-methylethylenediamine ($\mathbf{L_B}$ in Fig. 1) where either the linear *N*,*N*′-dimethylethylenediamine scaffold has been replaced with the cyclic piperazine ($\mathbf{L_A}$) or an additional maltol group has been inserted in place of a methyl group ($\mathbf{L_B}$).[29] These modifications deal with structural parameters such as stiffness, binding ability and steric hindrance of the molecule. Unfortunately, such compounds do not show improved performances compared to the lead compound; anyway, some hints could be gained concerning their biological activity. $\mathbf{L_A}$, notwithstanding its more rigid conformation, acts by a similar mechanism to Malten, being however less effective. $\mathbf{L_B}$ behaves instead differently from Malten, being able to induce mainly single strand breaks (nicks) of DNA and, at longer time of exposure and to a lesser extent, also double strand breaks. Therefore, even if the structural modifications brought on Malten negatively impact the biological activity, they result in an altered mechanism of action.[29]

Notwithstanding the structural modifications introduced, $\mathbf{L_A}$ and $\mathbf{L_B}$ possess binding properties towards transition metal ions similar to Malten, being able to form stable mononuclear

complexes. $\mathbf{L_B}$ was seen to give also metal complexes with different stoichiometries (2 : 1 and 3 : 2 metal to ligand ratio). Moreover, both ligands, in particular $\mathbf{L_A}$, are able to interact with rare earth cations.[29]

In this work, we aim to widen the maltol-based ligand family and study the effect of a different structural change introduced in the molecule of Malten, in particular on the maltol ring, both to gain further information about the molecular mechanism of action as well as to investigate the already known coordination properties of this family towards transition metal ions.[25] In particular, we followed our previous speculation on the maltol moiety being a Michael-type acceptor for nucleophilic sites of DNA, due to a partial positive charge at the C6 atom of maltol,[23d] which may explain the ability of the lead compounds to favor the covalent binding between DNA and proteins. To explore whether such a position plays a key role in the mechanism of action, two new maltol-based ligands decorated at C6 with two groups having different dimensions were synthesized.

Ligands **L1** (*N*,*N*′-bis((3-hydroxy-6-methyl-4-pyron-2-yl)methyl)-*N*,*N*′-dimethylethylenediamine) and **L2** (*N*,*N*′-bis((3-hydroxy-6-hydroxymethyl-4-pyron-2-yl)methyl)-*N*,*N*′-dimethylethylenediamine) possess, respectively, a methyl and a hydroxymethyl function at C6, that might prevent the involvement of maltol in the biological mechanism, inactivating the two compounds. Furthermore, the introduction of the hydroxyl group opens the way for the insertion of a fluorophore in this class of molecules, which could turn them from therapeutic to theranostic agents.

The two ligands were synthesized and characterized both in solution and in the solid state. The acid–base and stability properties of the free ligands were investigated by potentiometric, UV-VIS and NMR measurements. The crystal structure of diprotonated **L1** is reported and discussed. The coordination properties of both ligands in aqueous solution towards selected first row transition metal ions were also studied by potentiometric measurements. Finally, herein we reported the preliminary *in vitro* biological studies of the free ligands. All results obtained on **L1** and **L2** were compared with those of the precursor Malten to highlight the influence of the structural modifications at C6 on the ligand properties.

2. Experimental

2.1 General methods

UV/Vis absorption spectra were recorded at 298 K on a Varian Cary-100 spectrophotometer equipped with a temperature control unit. ^{1}H and ^{13}C NMR spectra were acquired on a Bruker AVANCE 400 spectrometer, operating at 400.13 and 100.61 MHz for ^{1}H and ^{13}C, respectively, and equipped with a variable-temperature controller. The temperature of the NMR probe was calibrated using 1,2-ethanediol as the calibration sample. For the spectra recorded in D_2O, the peak positions are reported with respect to HOD (δ = 4.75 ppm) for ^{1}H NMR spectra, while dioxane was used as the reference standard in ^{13}C NMR spectra (δ = 67.4 ppm). For the spectra recorded in $CDCl_3$ and DMSO the peak positions are referenced to residual solvent signals. ^{1}H–^{1}H and ^{1}H–^{13}C correlation experiments were performed to assign the signals. Chemical shifts (δ scale) are reported in parts per million (ppm values) relative to the characteristic peak of the solvent. ^{1}H NMR measurements to evaluate the stability of both **L1** and **L2** were performed at pH 7.4 in $H_2PO_4^-$/HPO_4^{2-} buffer.

2.2 X-ray crystallography

Intensity data for compound $[H_2\mathbf{L1}]\cdot(ClO_4)_2\cdot 2(H_2O)$ (**6**) were collected on an Oxford Diffraction Excalibur diffractometer using Mo K_α radiation (λ = 0.71069 Å). Data collection was performed at 100 K. The program CrysAlis v 1.171[30] was used to determine the cell parameters, to collect the intensity data and to reduce them. Intensities were corrected for Lorentz and polarization effects. Absorption correction was performed with the program ABSPACK implemented in CrysAlis. The structure of **6** was solved by using the SIR-2004 package[31] and subsequently refined on the F^2 values by the full-matrix least-squares program SHELXL-2018/3.[32] All the non-hydrogen atoms were anisotropically refined while all the hydrogen ones were found in the Fourier Synthesis and refined in accordance with the atom to which they are bound. The structure was solved as a twin by using the twinning law suggested by Platon.[33] Geometrical calculations were performed by PARST97[34] and molecular plots were produced by the Mercury 2.4[35] programs. Crystallographic data and refinement parameters are reported in Table S1 (ESI†). Deposition Number CCDC 2040416 contains the supplementary crystallographic data for this paper.†

2.3 EMF measurements

Equilibrium constants for protonation and complexation reactions of the two ligands were determined by pH-metric measurements in degassed 0.15 mol dm^{-3} NaCl at 298 ± 0.1 K, using the fully automatic equipment that has already been described.[36] An Ag/AgCl electrode in saturated KCl solution was employed as the reference electrode, while the glass electrode was calibrated as a hydrogen concentration probe through titration of known amounts of HCl with CO_2-free NaOH solutions. EMF data were acquired with the PASAT computer program.[37] The equivalent point, the standard potential E_o and the ionic product of water (pK_w = 13.73 ± 0.01 at 298.1 K in 0.1 M NaCl) were determined by using Gran's method.[38] At least three measurements (consisting of 100 data points for each) were performed for each system in the pH range of 2–11. In all experiments, the ligand concentration ([L]) was 1 × 10^{-3} mol dm^{-3}, while in complexation experiments a metal ion concentration of 0.8 [L] was employed. The computer program HYPERQUAD[39] was used to process the potentiometric data. Distribution diagrams were obtained by using the Hyss program.[40]

2.4 Synthesis

All chemicals were purchased in the highest quality commercially available. The solvents were of RP grade, unless otherwise indicated.

2-Chloromethyl-5-hydroxy-4*H*-pyran-4-one (2). A mixture of **1** (30.5 g; 0.215 mol) and $SOCl_2$ (70 ml) under a nitrogen atmosphere was stirred for 1 h. The precipitated yellow solid was

collected by filtration and washed with petroleum ether at 40–70 °C, to give **2** as a white powder (30 g, 87% yield). The crude product was pure enough to be used without further purification. ^{1}H NMR ($CDCl_3$, 25 °C): δ = 4.36 (s, 2H), 6.57 (s, 1H), 7.88 (s, 1H) ppm. ^{13}C NMR ($CDCl_3$, 25 °C): δ = 41.0, 111.9, 138.2, 145.8, 162.9, 173.9 ppm.

5-Hydroxy-2-methyl-4*H*-pyran-4-one (3). A solution of **2** (30 g, 0.187 mol) in distilled water (100 ml) was heated up to 50 °C and stirred till the color of the solution turned pink. Zn powder (24 g, 0.375 mol) was then added, followed by the dropwise addition of HCl(c), keeping the mixture at 70–80 °C. After 3 h the yellow mixture was filtered to remove the excess of Zn and then extracted with CH_2Cl_2 (5 × 200 ml). The combined organic layers were dried (Na_2SO_4), filtered and concentrated to give the crude product of **3** that was purified by recrystallization in 2-propanol, obtaining a light yellow powder (20.6 g, 87.5% yield). ^{1}H NMR ($CDCl_3$, 25 °C): δ = 2.32 (s, 3H), 6.29 (s, 1H), 7.79 (s, 1H) ppm. ^{13}C NMR ($CDCl_3$, 25 °C): δ = 20.1, 111.3, 137.6, 145.3, 166.6, 174.3 ppm.

***N*,*N*′-Bis((3-hydroxy-6-methyl-4-pyron-2-yl)methyl)-*N*,*N*′-dimethylethylenediamine dihydroperchlorate (L1·2HClO$_4$).** *N*,*N*′-Dimethylethylenediamine (0.305 g, 3.5 mmol) was added under a nitrogen atmosphere to a solution of 37% aqueous formaldehyde (0.580 ml; 7.8 mmol) in ethanol (2 ml). The mixture was stirred at room temperature for 30 min, then was added dropwise to an ethanolic solution of **3** (1.0 g, 7.1 mmol, in 15 ml EtOH). The mixture was vigorously stirred for 5 h, then a white solid precipitated that was filtered, washed with ethanol and dried. The crude product was purified by dissolution in ethanol and precipitation upon dropwise addition of a 10% perchloric acid ethanolic solution (0.931 g, 47% yield). (1.04 g, 47% yield, **L**·2HClO$_4$·4H$_2$O). ^{1}H NMR (D_2O, 25 °C): δ = 2.32 (s, 6H), 2.90 (s, 6H), 3.60 (s, 4H), 4.41 (s, 4H), 6.39 (s, 2H) ppm. ^{13}C NMR (D_2O, 25 °C): δ = 19.2, 40.9, 49.7, 52.3, 111.9, 140.6, 145.4, 169.0, 175.9 ppm. MS *m*/*z* (ESI): 365.4 (M + H$^+$). Anal. calcd for $C_{18}H_{34}Cl_2N_2O_{18}$: C, 33.92; H, 5.38; N, 4.40. Found: C, 34.1; H, 5.4; N, 4.6.

***N*,*N*′-Bis((3-hydroxy-6-hydroxymethyl-4-pyron-2-yl)methyl)-*N*,*N*′-dimethylethylenediamine (L2).** *N*,*N*′-Dimethylethylenediamine (0.16 g, 1.75 mmol) was added under a nitrogen atmosphere to a solution of 37% aqueous formaldehyde (0.32 ml; 4.30 mmol) in ethanol (2 ml). The mixture was stirred at room temperature for 30 min, then was added dropwise to an ethanolic solution of **1** (0.5 g, 3.85 mmol, in 10 ml EtOH). The mixture was vigorously stirred for 5 h, then a white solid precipitated that was filtered, washed with ethanol and dried (0.58 g, 84% yield). ^{1}H NMR (DMSO, 25 °C): δ = 2.21 (s, 6H), 2.55 (s, 4H), 3.57 (s, 4H), 4.28 (s, 4H), 6.30 (s, 2H) ppm. ^{13}C NMR (DMSO, 25 °C) δ = 42.49, 53.36, 54.42, 60.02, 109.37, 143.92, 147.64, 167.95, 174.01 ppm. MS *m*/*z* (ESI): 397.4 (M + H$^+$). Anal. calcd for $C_{18}H_{24}N_2O_8$: C, 54.54; H, 6.10; N, 7.07. Found: C, 54.4; H, 6.3; N, 7.0.

Caution: Perchlorate salts of organic compounds are potentially explosive; these compounds must be prepared and handled with care!

2.5 Biological studies

The immortalized promonocytic leukemia (U937) cell line was obtained from American Type Culture Collection (ATCC). Cells were grown in RPMI 1640 (Lonza) supplemented with 10% fetal bovine serum (FBS), 1% penicillin–streptomycin and 1% glutamine in a humidified atmosphere at 37 °C, as previously described.[41] **L1** and **L2** were dissolved at 1 mM in distilled water, as working solution, immediately before use. Treatments were carried out at the concentrations reported in the figures (cellular treatments performed at time 0′ and after 24 h) and cellular viability was evaluated after 48 h of treatment by Trypan blue dye exclusion assay (using CellDrop™ Automated Cell Counter – DeNovix) as previously described.[42] The data are reported as means (±SD) resulting from three independent experiments.

3. Results and discussion

3.1 Synthetic procedures

The two compounds *N*,*N*′-bis((3-hydroxy-6-methyl-4-pyron-2-yl)methyl)-*N*,*N*′-dimethylethylenediamine (**L1**) and *N*,*N*′-bis((3-hydroxy-6-hydroxymethyl-4-pyron-2-yl)methyl)-*N*,*N*′-dimethylethylenediamine (**L2**) were obtained starting from the commercially available 5-hydroxy-2-hydroxymethyl-4H-pyran-4-one (Kojic acid, **1** in Scheme 1). The current synthetic strategy offers the advantage of facile and fast preparation of the desired methylated and hydroxymethylated compounds, avoiding the protection and activation steps of maltol followed by SN_2 conditions that were employed in the synthesis of Malten.

As far as **L1** is concerned, the nucleophilic substitution of the hydroxyl group of kojic acid (**1**) with a chloride by using thionyl chloride gave compound **2**, which was then reduced by using Zn/HCl to give the methylated compound **3** in good yield. The Mannich reaction of compound **3** with aqueous formaldehyde (**4**) and *N*,*N*′-dimethylethylenediamine (**5**) provided ligand **L1** in one step (Scheme 1a).

First, formaldehyde (**4**) is reacted with the amine scaffold **5** in ethanol to give an intermediate diiminium cation, which is then added dropwise to an ethanolic solution of **3**. Crude **L1** precipitated as a white solid that was further purified by addition of a 10% perchloric acid ethanolic solution to give the desired compound as a yellowish dihydroperchlorate salt.

Ligand **L2** can be prepared even more easily by a single one-pot Mannich reaction starting directly from kojic acid (**1**), aqueous formaldehyde (**4**) and *N*,*N*′-dimethylethylenediamine (**5**), *via* formation of the intermediate diiminium cation (Scheme 1b). The product is achieved as a white solid, whose purity is good enough to allow the use of the compound as prepared. The commercial compounds **1**, **4** and **5** were used without any further purification.

3.2 Description of the structure

In the asymmetric unit of [H$_2$**L1**]·(ClO$_4$)$_2$·2(H$_2$O) (**6**) half of the [H$_2$**L1**]$^{2+}$ cation, one perchlorate anion and one molecule of water are present. The two halves of the diprotonated ligand are related by a center of symmetry ($-x$ + 1, $-y$, $-z$ + 1).

As can be seen in Fig. 3, the ligand takes an open wide conformation with the two aromatic rings (that lie on parallel planes, due to the presence of the center of symmetry) disposed

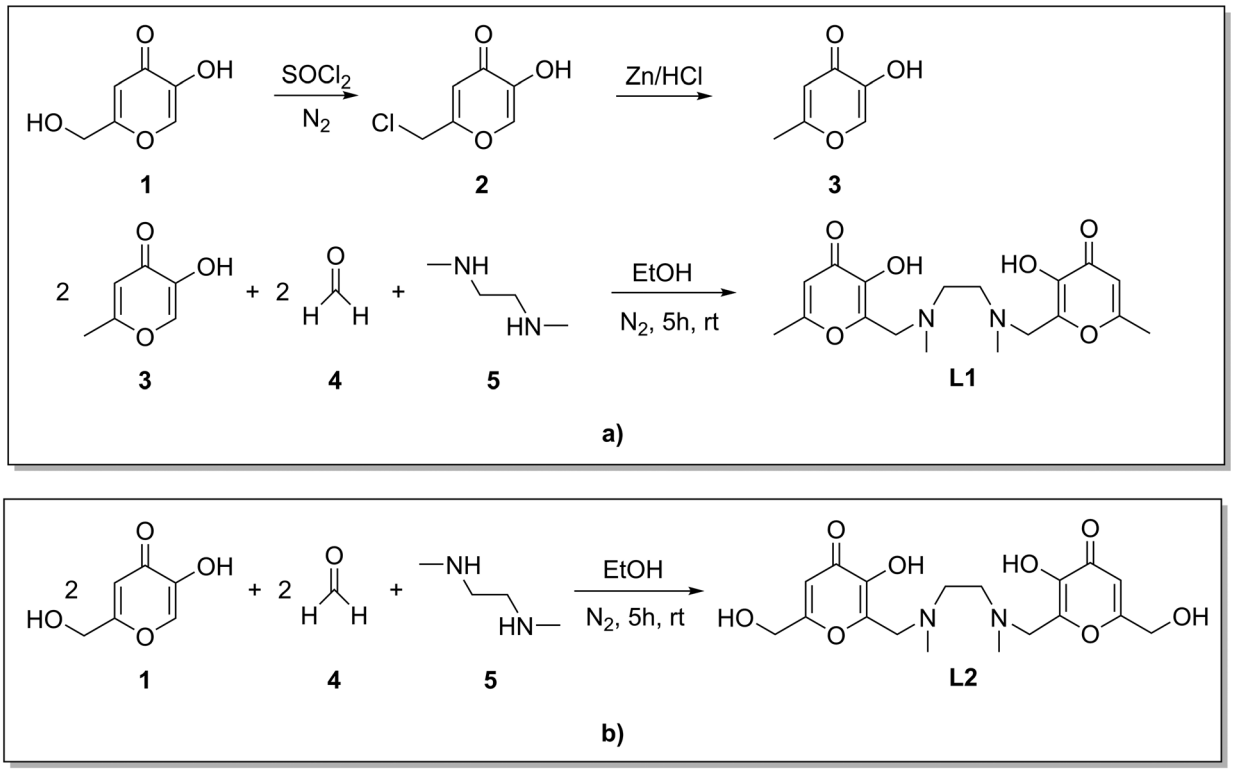

Scheme 1 Synthetic pathway for the preparation of ligands (a) **L1** and (b) **L2**.

on opposite sides with respect to the mean plane defined by the non-hydrogen atoms of the *N*,*N*′-dimethylethylenediamine chain.

The dihedral angles defining this chain have a sc/sc/ap/sc/sc conformation (sc: synclinal, ap: antiperiplanar) (Fig. S1, ESI†)[43] and the corresponding side arm orientation is o_Up-Down (Fig. S2, e, ESI†).[23d] Finally the angle between the mean plane defined by the atoms N1, C7, C7′, and N1′ (′ = $-x+1, -y, -z+1$; Fig. 3) and the mean plane containing the aromatic ring is 56.9(2)°.

The conformation taken by the ligand was compared with that of the parent compound Malten. As evidenced in Fig. 4, the conformation of the diprotonated **L1** ligand in **6** is well comparable with that observed in $[H_2Malten]\cdot(ClO_4)_2\cdot2(H_2O)$.[23d] In addition, the two compounds, *i.e.* $[H_2\mathbf{L1}]\cdot(ClO_4)_2\cdot2(H_2O)$ (**6**) and $[H_2Malten]\cdot(ClO_4)_2\cdot2(H_2O)$, are almost isomorphous and isostructural (see below).

In contrast, the conformation of the $[H_2\mathbf{L1}]^{2+}$ cation seen in the studied compound is quite different from that observed for the parent ligand $[H_2Malten]^{2+}$ in the $[H_2Malten]\cdot[PtCl_4]\cdot2H_2O$ platinum complex,[44] where the chain connecting the two maltol units takes a sc/ap/ap/ap/sc conformation, the overall disposition of the cation still being o_Up-Down (Fig. 5).

In the crystal packing of **6** some strong H-bond and π–π interactions are present.[45] Due to the presence of the latter, two symmetry related ($-x+2, -y+1, -z+1$) $[H_2Malten]^{2+}$ cations are linked together and parallel chains form (the distance between the mean planes containing the interacting rings is 3.311(4) Å, while the distance between the two centroids is 3.578(5) Å) (Fig. S3, ESI†).

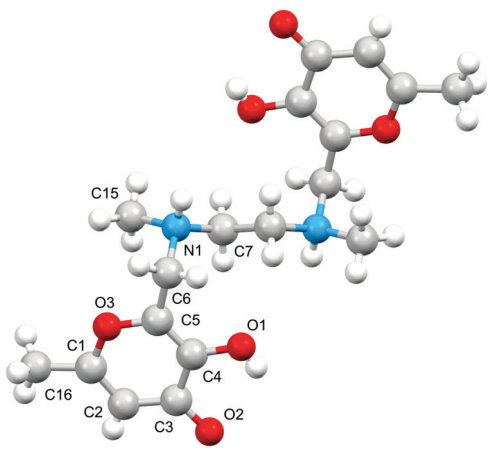

Fig. 3 Ball and stick view of the ligand cation $[H_2\mathbf{L1}]^{2+}$ in **6**.

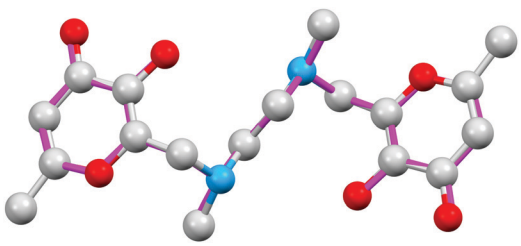

Fig. 4 Superimposition of the $[H_2\mathbf{L1}]^{2+}$ (ball and stick) and $[H_2Malten]^{2+}$ (as found in the $[H_2Malten]\cdot(ClO_4)_2\cdot2(H_2O)$[23d] compound, stick, magenta) cations (RMS: 0.121 Å).

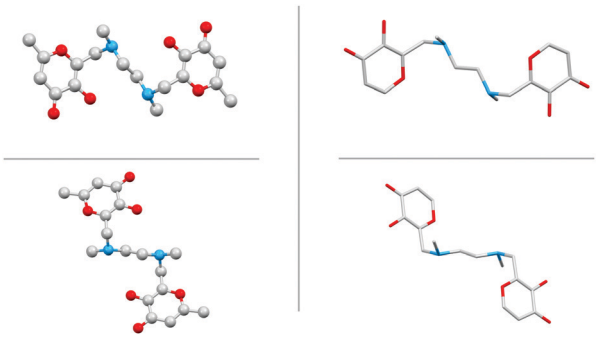

Fig. 5 Conformation taken by $[H_2\mathbf{L1}]^{2+}$ in **6** (ball and stick) and by $[H_2Malten]^{2+}$ in $[H_2Malten]\cdot[PtCl_4]\cdot 2H_2O$[44] (stick).

Table 1 Selected intermolecular hydrogen bonds in compound **6**

D–H···A	D···A (Å)	H···A (Å)	X–H···A (°)
O1w–H1wb···O11	3.100(5)	2.36(7)	153(7)
O1–H1o···O11	2.770(5)	2.08(6)	163(6)
O1w–H1wb···O2	3.049(4)	2.51(5)	126(6)
N1–H1n···O2[a]	2.689(5)	1.73(6)	174(5)
C6–H6a···O1w[a]	3.239(6)	2.43(6)	140(4)
C15–H15c···O14[b]	3.362(5)	2.48(5)	160(5)
C15–H15b···O14[c]	3.385(6)	2.47(7)	167(5)

[a] $x-1, +y, +z$. [b] $-x+1, -y, -z+1$. [c] $-x+2, -y, -z+1$.

These chains are linked together by means of H-bond interactions involving the hydrogen atom bonded to N1 and the oxygen atom O2 of a symmetry related $[H_2\mathbf{L1}]^{2+}$ cation ($x-1$, $+y$, $+z$) (see Fig. 3 for the atom labelling). Due to such interactions, planes perpendicular to the *c* axis form.

Finally, the water molecules and the perchlorate anions are located between such planes and interact with them by means of H-bonds (see Fig. S4 (ESI†) and Table 1).

3.3 Acid–base behavior

The acid–base behavior of **L1** and **L2** was investigated by both potentiometric and UV-Vis measurements.

The basicity constants of **L1** and **L2** were potentiometrically determined in 0.15 M NaCl aqueous solution at 298.1 K and are summarized in Table 2. Both neutral ligands behave as diprotic acids and bases under the used experimental conditions. They are able indeed to add up to two protons, reaching the $H_2\mathbf{L}^{2+}$ species, and they can be present in solution as anionic $H_{-2}\mathbf{L}^{2-}$ species.

Table 2 Protonation constants ($\log K$) of **L1** and **L2** potentiometrically determined in 0.15 mol dm^{-3} NaCl aqueous solution at 298.1 K

	$\log K$	
Reaction	**L** = **L1**	**L** = **L2**
$H_{-2}\mathbf{L}^{2-} + H^+ = H_{-1}\mathbf{L}^-$	9.13(8)[a]	8.70(7)
$H_{-1}\mathbf{L}^- + H^+ = \mathbf{L}$	8.37(9)	7.72(7)
$\mathbf{L} + H^+ = H\mathbf{L}^+$	6.98(7)	6.14(9)
$H\mathbf{L}^+ + H^+ = H_2\mathbf{L}^{2+}$	3.90(8)	3.09(9)

[a] Values in parentheses are the standard deviations on the last significant figure.

The analysis of the protonation constants starting from the anionic $H_{-2}\mathbf{L}^{2-}$ species reveals that **L1** and **L2** behave very similarly to each other, although **L1** shows a slightly higher $\log k$ value for each protonation step than **L2**. Both ligands exhibit a quite linear decrease in basicity up to the addition of the third proton, with $\log K$ values ranging from 9.13 to 6.98 and 8.70 to 6.14 for **L1** and **L2**, respectively. The last protonation step is associated with a drop of 3 logarithmic units ($\log K_4 = 3.90$ and 3.09, respectively); this can be justified by the electrostatic repulsion occurring between the two closely spaced ammonium groups in the $H_2\mathbf{L}^{2+}$ species, suggesting the involvement of the diamine moiety in this last protonation step.

The values and trend of the basicity constants are comparable with those of the previously reported bis-maltol-diamine ligands belonging to this family,[23d,29] and in particular with those of the parent ligand Malten.[23d]

More in detail, **L1** and **L2** behave very similar to Malten towards proton addition, even if values for **L1** and **L2** are a little higher and a little lower, respectively, than Malten for each protonation step. The modification introduced in the molecular structure of Malten refers to the substituent at the carbon atom C6 of the maltol ring, thus a positive and a negative inductive effect of the methyl and hydroxymethyl substituents at C6 for **L1** and **L2**, respectively, with respect to the H atom in Malten, may be invoked to explain this little difference in their basicity. In other words, the different electronic density on the maltol ring caused by the presence of different groups on the C6 atom slightly affects the basicity of the compounds.

Starting from the $H_2\mathbf{L}^{2+}$ species and looking at the molecular site in each protonation step, the comparison of the basicity constant values suggests the involvement of a nitrogen atom of the ethylenediamine fragment in the first step ($\log K = 10.16$ for *N*,*N*′-dimethylethylenediamine[46]), followed by the protonation of the two maltolate functions ($\log K = 8.44$ for free deprotonated maltol[47]) and of the second nitrogen atom of the diamine scaffold, at last.

Fig. 6 shows the distribution diagrams of the protonated species of **L1** and **L2** together with the trend of the absorbance at 316 and 323 nm for **L1** and **L2**, respectively, in aqueous solution as a function of pH (*vide infra*). It is to highlight that at physiological pH = 7.4, although the neutral **L** species is the main one for both **L1** and **L2**, other species coexist in solution for both systems.

UV-Vis absorption electronic measurements in aqueous solution support the species suggested by potentiometric measurements (*i.e.* the sites involved in the protonation), therefore allowing to know not only the species present in solution at the different pH values but also the acidic proton distribution exploiting the presence of the maltol chromophore (Fig. 7).

Spectrophotometrically, **L1** and **L2** behave very similarly to one another, showing at pH 2, where the fully protonated $H_2\mathbf{L}^{2+}$ species is present in solution, a band with λ_{max} = 270 and 275 nm (ε = 16 700 and 17 400 cm^{-1} mol^{-1} dm^3), respectively, that keeps lowering upon increasing the pH, while a new band

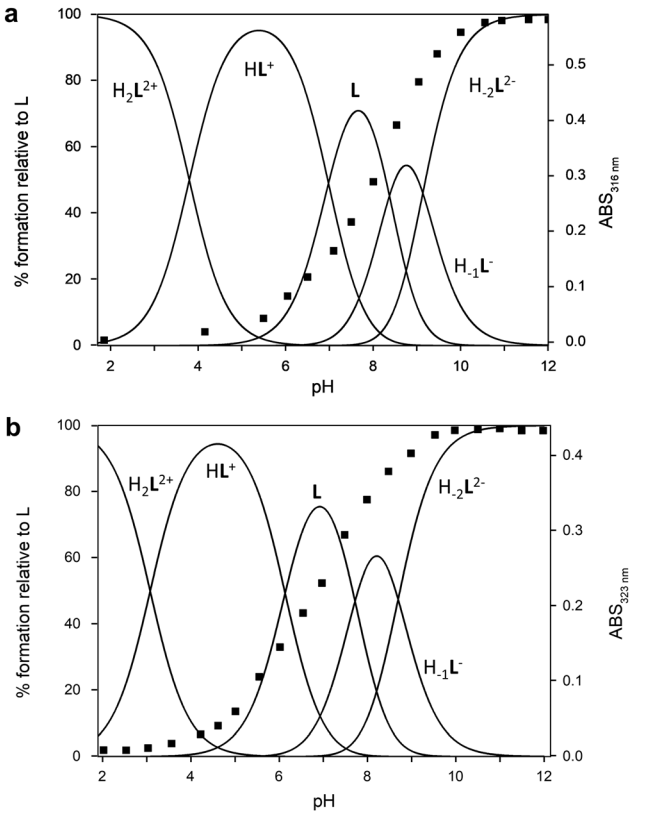

Fig. 6 Distribution diagram of the species (–) and trend of the absorbance (■) for (a) **L1** (λ = 316 nm) and (b) **L2** (λ = 323 nm) in aqueous solution as a function of pH. UV-Vis measurements: [**L1**] = [**L2**] = 5×10^{-5} mol dm^{-3}; potentiometric measurements: [**L1**] = [**L2**] = 1×10^{-3} mol dm^{-3}, I = 0.15 mol dm^{-3} NaCl, T = 298.1 K.

grows, starting from pH 5, with λ_{max} = 316 and 323 nm, respectively, and reaches its maximum in both cases at pH 10 (ε = 11 200 and 8600 cm^{-1} mol^{-1} dm^3), where the $H_{-2}L^{2-}$ species prevails in solution (Fig. 6). The band at higher energy is related to the presence of maltol groups in their neutral form, while that at lower energy indicates the occurrence of the deprotonation of such functions.

In the case of **L2**, the deprotonation starts at a slightly lower pH value than for **L1** (Fig. 6), in agreement with the acidity of **L2** being slightly higher than that of **L1**. Overall it seems that the small structural variations introduced in the Malten molecule to give ligands **L1** and **L2** do not significantly alter either the acid–base behavior or the protonated species present in solution at the different pH values. However, the different groups present in the three systems on the carbon atom C6 of maltol, *i.e.* H in Malten, $-CH_3$ in **L1** and $-CH_2OH$ in **L2**, little affect the absorptivity in the species.

Analogously to all other members of the maltol-based ligand family, the observed absorption behavior is in line with the potentiometric studies and suggests the involvement of amine functions in the first and last protonation steps, where the $H_{-2}L^{2-}$ and HL^+ species undergo the protonation; in the remaining steps the maltolate groups are engaged in the protonation, which involves the $H_{-1}L^-$ and **L** species to afford the **L** and H_1L^+ ones, respectively.

Potentiometric and UV-Vis data overall suggest for **L1** and **L2** the protonation scheme reported in Fig. 8. In the case of **L1**, three species are present at a physiological pH of 7.4, with the zwitterionic form **L** greatly prevailing on the cationic form HL^+ and on the anionic form $H_{-1}L^-$ (70 *vs.* 20 *vs.* 10%); in the case of **L2**, two species are present at pH 7.4, with the zwitterionic form **L** almost doubling the anionic form $H_{-1}L^-$ (60 *vs.* 35%). In both cases, the zwitterionic form **L** can be considered as the main species present in the biological medium at such pH, similarly to that found for Malten.

3.4 Coordination of metal cations

The binding properties of **L1** and **L2** towards Cu(II), Zn(II) and Co(II) transition metal ions were investigated by potentiometric measurements in 0.15 M NaCl aqueous solution at 298.1 K. The stability constants for the complexation reactions of **L1** and **L2** with the three cations are reported in Table 3, while Fig. 9

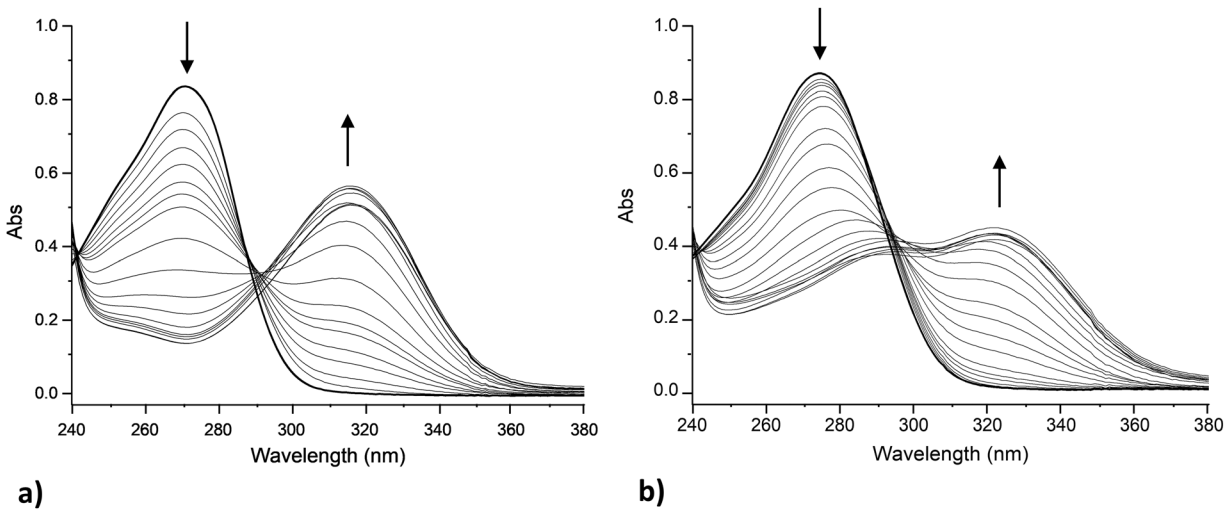

Fig. 7 Absorption spectra in the UV-Vis range of (a) **L1** and (b) **L2** in aqueous solution as a function of pH. [**L1**] = [**L2**] = 5×10^{-5} mol dm^{-3}.

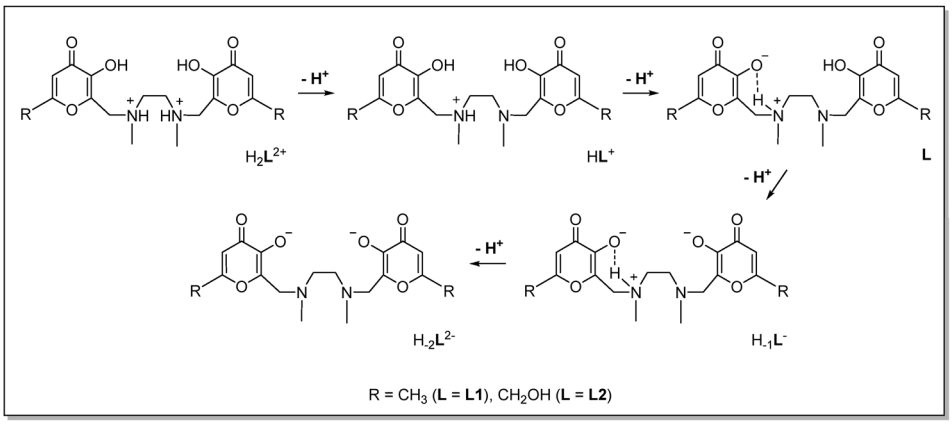

Fig. 8 Location of acidic hydrogen atoms in the protonated species of **L1** and **L2**.

shows the distribution diagrams of the species for the **L**–M(II) systems (**L** = **L1**, **L2**; M(II) = Cu(II), Zn(II), Co(II)) as a function of pH.

Both ligands are able to form stable mononuclear $[M(H_{-2}L)]$ complexes with all studied metal ions, whose formation constant values agree with the Irving–Williams series (Table 3). Complexes having different stoichiometries were not found under the present experimental conditions.

In all cases, the neutral $[M(H_{-2}L)]$ species is the one prevailing in solution in a wide range of pH (5–10); in some cases the pH interval is even wider, starting at lower values (around 4, in the case of Cu(II) with both ligands) and/or ending at higher values (around 11 in the case of Cu(II) and Co(II) with both ligands) (Fig. 9).

Within the series of the diamino-bis-maltol ligands (Malten, L_A, **L1**, **L2**), **L1** always provides the highest constant values for the addition of Cu(II), Zn(II) and Co(II) (Table 3 and ref. 29). These data suggest that the insertion of the electron-donor methyl group at C6 positively affects the binding properties of the ligand.

In contrast, the insertion of the hydroxymethyl group in **L2** produces an opposite effect compared to the methyl group, all stability constants being lower than those of **L1** for all M(II) ions investigated. Moreover, stability values for complex **L2** fluctuate around those for Malten complexes.

Based on equilibrium constant values, an analogous coordination environment around the M(II) ion of both ligands could be hypothesized. Looking at the crystal structures of Malten and at previous studies,[25a,25b,25d,28,29] a N_2O_2 environment may be suggested, coming from two oxygen atoms of the deprotonated maltol functions of **L1** and **L2** along with two nitrogen atoms of the polyamine (Fig. 10).

In both **L1** and **L2** the $[Cu(H_{-2}L)]$ species can add a proton to form the $[Cu(H_{-1}L)]^+$ cation, with addition constant values ascribable to the protonation of a donor atom involved in the Cu(II) coordination; once again, the value for the proton addition is slightly higher for **L1** than for **L2**.

Lastly, all $[M(H_{-2}L)]$ species are able to form monohydroxylated $[M(H_{-2}L)OH]^-$ species with all the tested metal ions; also in this case, the addition values for **L1** are higher than for **L2**.

The comparison with Malten shows that both proton and hydroxyl addition values are slightly higher for **L1** than for Malten except in the case of the addition of OH^- to the Co(II) complex ($\log K_{\mathbf{L1}} = 2.58$, $\log K_{\mathrm{Malten}} = 2.92$[25a]).

3.5 Stability studies and biological data

^{1}H NMR experiments were performed to gain insight into the stability of **L1** and **L2** in aqueous solution. Time-course analysis of buffered solutions of the two ligands (phosphoric buffer, pH 7.4) allowed the determination of the degradation time of **L1** and **L2** thanks to the integration of peak areas in ^{1}H NMR spectra. In particular, the time required for 50% degradation is 4 hours and 5 hours 30 min for **L1** and **L2**, respectively; in both cases, the degradation process is far faster than for Malten (10 h), $\mathbf{L_A}$ (10 h) and $\mathbf{L_B}$ (48 h).

Table 3 Logarithms of the equilibrium constants determined in 0.15 mol dm^{-3} NaCl at 298.1 K for the complexation reactions of **L1** and **L2** with Cu(II), Zn(II) and Co(II) cations

	$\log K$					
	Cu(II)		Zn(II)		Co(II)	
Reaction	**L** = **L1**	**L** = **L2**	**L** = **L1**	**L** = **L2**	**L** = **L1**	**L** = **L2**
$M^{2+} + H_{-2}L^{2-} = [M(H_{-2}L)]$	19.02(8)[a]	17.07(3)	12.31(7)	10.44(7)	11.75(8)	10.36(5)
$[M(H_{-2}L)] + H^+ = [M(H_{-1}L)]^+$	4.40(9)	3.55(3)	—	—	—	—
$[M(H_{-2}L)] + OH^- = [M(H_{-2}L)OH]^-$	3.31(7)	2.71(5)	3.60(8)	3.3(1)	2.58(7)	2.57(7)

[a] Values in parentheses are the standard deviations on the last significant figure.

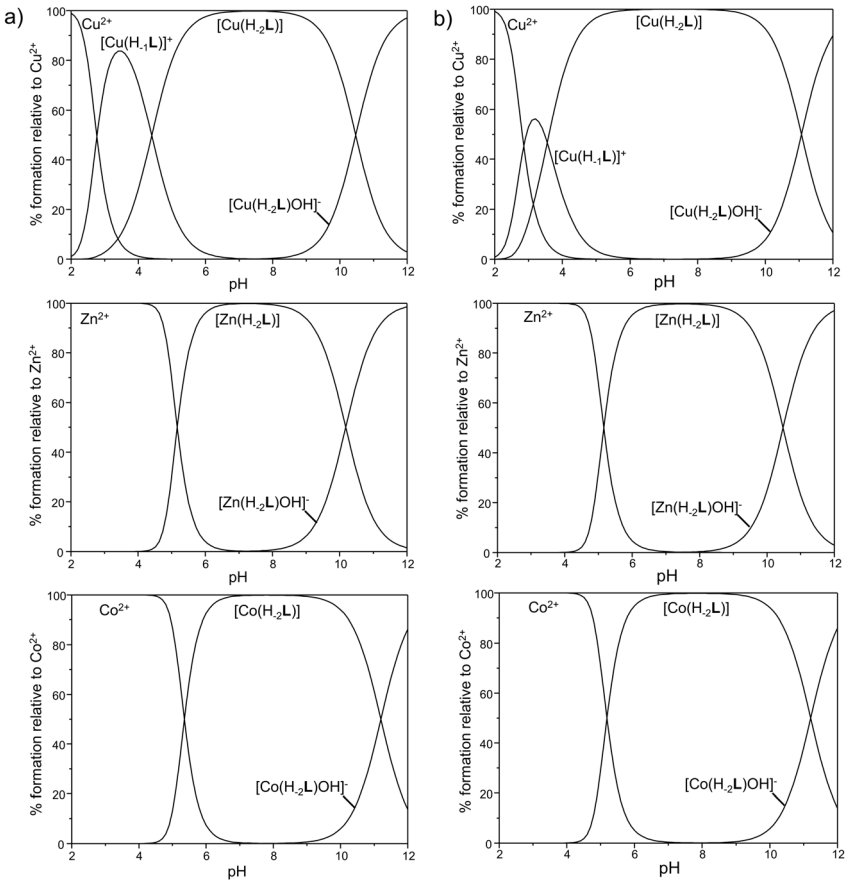

Fig. 9 Distribution diagram of the species for **L**–M(II) systems (M(II) = Cu(II), Zn(II) and Co(II)) in 1 : 1 molar ratio as a function of pH in aqueous solution. (a) **L** = **L1**; (b) **L** = **L2**. [**L1**] = [**L2**] = [Cu(II)]/[Zn(II)]/[Co(II)] = 1×10^{-3} mol dm^{-3}, I = 0.15 mol dm^{-3} NaCl, T = 298.1 K.

Thus, even if the introduced structural variations do not significantly affect the acid–base properties, the substitution at C6 clearly makes the ligands more susceptible to degradation.

The potential of **L1** and **L2** to alter the biological properties of human cells was monitored exploiting the promonocytic leukemia (U937) cell line, a cellular model already used to test the biological properties of other maltol-based polyamine ligands including Malten.[23c,d,29] In order to evaluate the potential biological activity, treatments (at doses from 5 to 100 μM) were conducted with **L1** and **L2** always in parallel to the reference ligand Malten (Fig. 11).

Malten, used as control was able to strongly decrease the cell survival, reaching values close to zero at the highest dose tested (100 μM), coherently as already reported.[23c,23d,29] A different behavior can be observed treating the cells with **L1** and **L2**. In

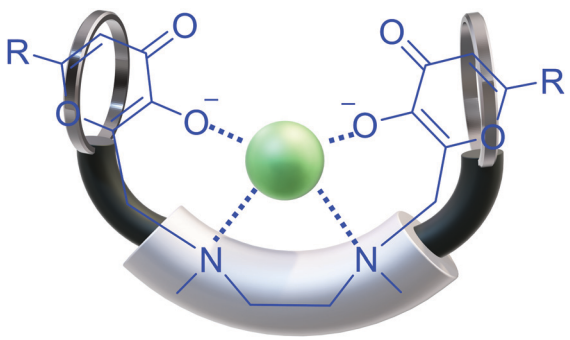

Fig. 10 Scheme proposed for the coordination of M(II) ions (M(II) = green sphere = Cu(II)Cu(II), Zn(II) and Co(II)) by **L1** and **L2** (R = CH_3, for **L1**; CH_2OH for **L2**).

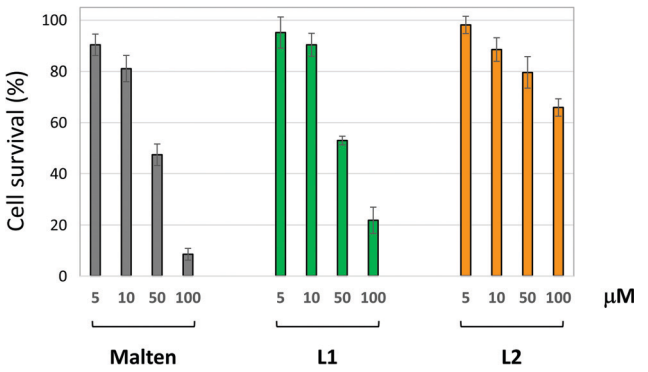

Fig. 11 Dose-dependent biological activity of **L1** and **L2**. Cell viability of U937 promonocytic leukemia was measured by Trypan blue dye exclusion assay (number of Trypan blue negative cells) after 48 h of treatments. Values are reported as means ± SDs of three independent experiments.

fact, both **L1** and **L2** showed a lower biological effect with respect to that observed with Malten, at all doses tested.

However, **L1** demonstrated a more efficient biological activity compared to **L2** at higher doses (50–100 μM) (Fig. 11).

The higher effect shown by **L1** with respect to **L2** is in agreement with the induction of cell death monitored at 100 μM (≃70% for **L1** and ≃15% for **L2**). The cytotoxic effects of Malten, instead, are induced at a dose of 50 μM (≃20%) and, more efficiently, at 100 μM (≃90%).

4 Conclusions

In this paper we continued our ongoing studies on maltol-based ligands by further expanding the family through the synthesis of two new compounds, which bear a methyl- (**L1**) or hydroxymethyl substituent (**L2**) at the C6 position of the maltol ring. The study was aimed at better investigating the role of such a position in the biological mechanism of action, which is known to involve complex structural alterations of genomic DNA possibly induced by DNA intermolecular crosslinking.

The solid state analysis revealed that, compared to the lead compound Malten, no differences are retrieved following the substitution with the methyl group at C6 in terms of the molecular conformation or crystal packing; in the same way, solution studies disclosed an acid–base behavior similar to Malten for both **L1** and **L2** ligands. However, both shorter degradation time and better binding properties towards Cu(II), Zn(II) and Co(II), especially in the case of **L1**, were found, suggesting a possible electronic influence of the two introduced substituent groups. From a structural point of view, the introduction of a hydroxymethyl group at C6 seems sufficient to largely impair the biological activity of the lead compound (Malten), returning a higher cell survival for **L2** compared to both **L1** and Malten, perhaps following a reactivity lowering toward nucleophilic attack due to increased steric hindrance at C6. However, the residual biological activity exerted by **L2** does not support entirely the hypothesized role of the C6 position in the supposed DNA (or DNA–protein) crosslinking. In addition, the shorter degradation time of **L1** and **L2** with respect to Malten is a phenomenon that has to be considered in order to explain the reduced biological activity observed, in particular for **L2**.

Conflicts of interest

There are no conflicts to declare.

Acknowledgements

The authors thank the Italian Ministero dell'Istruzione dell'-Università e della Ricerca (MIUR) (project 20173X8WA4 and project 2017EKCS35), the University of Urbino (Department of Pure and Applied Sciences – Grant DISPEA FUSI PROG2019, DISPEA GIORGI PROG2020) and the Fondazione ''Francesca Pirozzi''.

Notes and references

1 M. J. Thun, J. O. DeLancey, M. M. Center, A. Jemal and E. M. Ward, *Carcinogenesis*, 2010, **31**, 100–110.
2 Joint FAO/WHO Expert Committee on Food Additives, *W. H. O. Tech. Rep. Ser.*, 2006, **939**, 1–80.
3 R. S. Harvey, D. M. Reffitt, L. A. Doig, J. Meenan, R. D. Ellis, R. P. H. Thompson and J. J. Powell, *Aliment. Pharmacol. Ther.*, 1998, **12**, 845–848.
4 K. H. Thompson, B. D. Liboiron, Y. Sun, K. D. D. Bellman, I. A. Setyawati, B. O. Patrick, V. Karunaratne, G. Rawji, J. Wheeler, K. Sutton, S. Bhanot, C. Cassidy, J. H. McNeill, V. G. Yuen and C. Orvig, *J. Biol. Inorg. Chem.*, 2003, **8**, 66–74.
5 V. Krishnakumar, D. Barathi, R. Mathammal, J. Balamani and N. Jayamani, *Spectrochim. Acta, Part A*, 2014, **121**, 245–253.
6 A. Anwar-Mohamed and A. O. El-Kadi, *Toxicol. In Vitro*, 2007, **21**, 685–690.
7 (*a*) B. Song, K. Saatchi, G. H. Rawji and C. Orvig, *Inorg. Chim. Acta*, 2002, **339**, 393–399; (*b*) K. Saatchi, K. H. Thompson, B. O. Patrick, M. Pink, V. G. Yuen, J. H. McNeill and C. Orvig, *Inorg. Chem.*, 2005, **44**, 2689–2697.
8 (*a*) M. Hironishi, R. Kordek, R. Yanagihara and R. M. Garruto, *Neurodegeneration*, 1996, **5**, 325–329; (*b*) E. Yasumoto, K. Nakano, T. Nakayachi, S. R. Morshed, K. Hashimoto, H. Kikuchi, H. Nishikawa, M. Kawase and H. Sakagami, *Anticancer Res.*, 2004, **24**, 755–762; (*c*) K. Murakami, K. Ishida, K. Watakabe, R. Tsubouchi, M. Haneda and M. Yoshino, *BioMetals*, 2006, **19**, 253–257; (*d*) K. Murakami, K. Ishida, K. K. Watakabe, R. Tsubouchi, M. Naruse and M. Yoshino, *Toxicol. Lett.*, 2006, **161**, 102–107.
9 Y. L. Hong, H. Z. Pan, M. D. Scott and S. R. Meshnick, *Free Radical Biol. Med.*, 1992, **12**, 213–218.
10 Y. B. Kim, S. H. Oh, D. E. Sok and M. R. Kim, *Nutr. Neurosci.*, 2004, **7**, 33–39.
11 Y. Yang, J. Wang, C. Xu, H. Pan and Z. Zhang, *J. Biochem. Mol. Biol.*, 2006, **39**, 145–149.
12 W. Kandioller, C. G. Hartinger, A. A. Nazarov, C. Bartel, M. Skocic, M. A. Jakupec, V. B. Arion and B. K. Keppler, *Chemistry*, 2009, **15**, 12283–12291.
13 O. Domotor, S. Aicher, M. Schmidlehner, M. S. Novak, A. Roller, M. A. Jakupec, W. Kandioller, C. G. Hartinger, B. K. Keppler and E. A. Enyedy, *J. Inorg. Biochem.*, 2014, **134**, 57–65.
14 (*a*) J. Bransovà, J. Brtko, M. Uher and L. Novotny, *Int. J. Cell Biol.*, 1995, **7**, 701–706; (*b*) M. A. Jakupec and B. K. Keppler, *Curr. Top. Med. Chem.*, 2004, **4**, 1575–1583; (*c*) A. Barve, A. Kumbhar, M. Bhat, B. Joshi, R. Butcher, U. Sonawane and R. Joshi, *Inorg. Chem.*, 2009, **48**, 9120–9132; (*d*) W. Kandioller, C. G. Hartinger, A. A. Nazarov, J. Kasser, R. John, M. A. Jakupec, V. B. Arion, P. J. Dyson and B. K. Keppler, *J. Organomet. Chem.*, 2009, **694**, 922–929.
15 T. Thomas and T. J. Thomas, *J. Cell. Mol. Med.*, 2003, **7**, 113–126.
16 H. M. Wallace, A. V. Fraser and A. Hughes, *Biochem. J.*, 2003, **376**, 1–97.

17 H. M. Wallace and K. Niiranen, *Amino Acids*, 2007, **33**, 261–265.
18 A. V. Fraser, P. M. Woster and H. M. Wallace, *Biochem. J.*, 2002, **367**, 307–312.
19 S. M. Oredsson, K. Alm, E. Dahlberg, C. M. Holst, V. M. Johansson, L. Myhre and E. Soderstjerna, *Biochem. Soc. Trans.*, 2007, **35**, 405–409.
20 W. E. Criss, *Turk. J. Med. Sci.*, 2003, **33**, 195–205.
21 H. A. Hahm, V. R. Dunn, K. A. Butash, W. L. Deveraux, P. M. Woster, R. A. Casero, Jr. and N. E. Davidson, *Clin. Cancer Res.*, 2001, **7**, 391–399.
22 A. Pledgie-Tracy, M. Billam, A. Hacker, M. D. Sobolewski, P. M. Woster, Z. Zhang, R. A. Casero and N. E. Davidson, *Cancer Chemother. Pharmacol.*, 2010, **65**, 1067–1081.
23 (*a*) M. Fanelli and V. Fusi, *PCT Int. Appl.*, WO 2010061282A1 20100603, 2010; (*b*) M. Fanelli and V. Fusi, Ital., IT 1392249 B1 20120222, 2012; (*c*) S. Amatori, I. Bagaloni, M. Fanelli, M. Formica, V. Fusi, L. Giorgi and E. Macedi, *Br. J. Cancer*, 2010, **103**, 239–248; (*d*) S. Amatori, G. Ambrosi, M. Fanelli, M. Formica, V. Fusi, L. Giorgi, E. Macedi, M. Micheloni, P. Paoli, R. Pontellini and P. Rossi, *J. Org. Chem.*, 2012, **77**, 2207–2218.
24 C. Guerzoni, S. Amatori, L. Giorgi, M. C. Manara, L. Landuzzi, P.-L. Lollini, A. Tassoni, M. Balducci, M. Manfrini, L. Pratelli, M. Serra, P. Picci, M. Magnani, V. Fusi, M. Fanelli and K. Scotlandi, *BMC Cancer*, 2014, **14**, 137.
25 (*a*) C. Benelli, E. Borgogelli, M. Formica, V. Fusi, L. Giorgi, E. Macedi, M. Micheloni, P. Paoli and P. Rossi, *Dalton Trans.*, 2013, **42**, 5848–5859; (*b*) S. Amatori, G. Ambrosi, M. Fanelli, M. Formica, V. Fusi, L. Giorgi, E. Macedi, M. Micheloni, P. Paoli and P. Rossi, *Chem. – Eur. J.*, 2014, **20**, 11048–11057; (*c*) P. Rossi, E. Macedi, P. Paoli, L. Giorgi, M. Formica and V. Fusi, *Acta Crystallogr., Sect. E: Crystallogr. Commun.*, 2017, **73**, 1959–1965; (*d*) P. Rossi, S. Ciattini, M. Formica, V. Fusi, L. Giorgi, E. Macedi, M. Micheloni and P. Paoli, *Inorg. Chim. Acta*, 2018, **470**, 254–262.
26 E. Borgogelli, M. Formica, V. Fusi, L. Giorgi, E. Macedi, M. Micheloni, P. Paoli and P. Rossi, *Dalton Trans.*, 2013, **42**, 2902–2912.
27 P. Paoli, E. Macedi, P. Rossi, L. Giorgi, M. Formica and V. Fusi, *Acta Crystallogr., Sect. E: Crystallogr. Commun.*, 2017, **E73**, 1806–1811.
28 P. Rossi, E. Macedi, M. Formica, L. Giorgi, P. Paoli and V. Fusi, *ChemPlusChem*, 2020, **85**, 1179–1189.
29 E. Macedi, D. Paderni, M. Formica, L. Conti, M. Fanelli, L. Giorgi, S. Amatori, G. Ambrosi, B. Valtancoli and V. Fusi, *Molecules*, 2020, **25**, 943.
30 *CrysAlisPro 1.171.38.41r (Rigaku Oxford Diffraction)*, 2015.
31 M. C. Burla, R. Caliandro, M. Camalli, B. Carrozzini, G. L. Cascarano, L. De Caro, C. Giacovazzo, G. Polidori and R. Spagna, *J. Appl. Crystallogr.*, 2005, **38**, 381–388.
32 G. M. Sheldrick, *Acta Crystallogr., Sect. C: Struct. Chem.*, 2015, **71**, 3–8.
33 A. L. Speck, *Acta Crystallogr., Sect. D: Biol. Crystallogr.*, 2009, **65**, 148–155.
34 M. Nardelli, *J. Appl. Cryst.*, 1995, **28**, 659–662.
35 C. F. Macrae, I. J. Bruno, J. A. Chisholm, P. R. Edgington, P. McCabe, E. Pidcock, L. Rodriguez-Monge, R. Taylor, J. van de Streek and P. A. Wood, *J. Appl. Cryst.*, 2008, **41**, 466–470.
36 (*a*) F. Bartoli, A. Bencini, L. Conti, C. Giorgi, B. Valtancoli, P. Paoli, P. Rossi, N. Le Bris and R. Tripier, *Org. Biomol. Chem.*, 2016, **14**, 8309–8321; (*b*) M. C. Aragoni, M. Arca, A. Bencini, C. Caltagirone, L. Conti, A. Garau, B. Valtancoli, F. Isaia, V. Lippolis, F. Palomba, L. Prodi and N. Zaccheroni, *Supramol. Chem.*, 2017, **29**, 912–921; (*c*) R. Montis, A. Bencini, S. J. Coles, L. Conti, L. Fusaro, P. A. Gale, C. Giorgi, P. N. Horton, V. Lippolis, L. K. Mapp and C. Caltagirone, *Chem. Commun.*, 2019, **55**, 2745–2748; (*d*) F. Bettazzi, D. Voccia, A. Bencini, C. Giorgi, I. Palchetti, B. Valtancoli and L. Conti, *Eur. J. Inorg. Chem.*, 2018, 2675–2679; (*e*) L. Conti, A. Bencini, C. Ferrante, C. Gellini, P. Paoli, M. Parri, G. Pietraperzia, B. Valtancoli and C. Giorgi, *Chem. – Eur. J.*, 2019, **25**, 10606–10615.
37 F. J. Rossotti and H. Rossotti, *J. Chem. Educ.*, 1965, **42**, 375–378.
38 G. Gran, *Analyst*, 1952, **77**, 661.
39 P. Gans, A. Sabatini and A. Vacca, *Talanta*, 1996, **43**, 1739–1753.
40 L. Alderighi, P. Gans, A. Ienco, D. Peters, A. Sabatini and A. Vacca, *Coord. Chem. Rev.*, 1999, **184**, 311–318.
41 S. Amatori, G. Ambrosi, M. Fanelli, M. Formica, V. Fusi, L. Giorgi, E. Macedi, M. Micheloni, P. Paoli, R. Pontellini, P. Rossi and M. A. Varrese, *Chem. – Eur. J.*, 2012, **18**, 4274–4284.
42 S. Amatori, G. Ambrosi, A. E. Provenzano, M. Fanelli, M. Formica, V. Fusi, L. Giorgi, E. Macedi, M. Micheloni, P. Paoli and P. Rossi, *J. Inorg. Biochem.*, 2016, **162**, 154–161.
43 G. P. Moss, *Pure Appl. Chem.*, 1996, **68**, 2193–2222.
44 V. Fusi, L. Giorgi, E. Macedi, P. Paoli and P. Rossi, *Acta Crystallogr., Sect. E: Struct. Rep. Online*, 2012, **68**, m1323–m1324.
45 G. R. Desiraju and T. Steiner, *The weak hydrogen bond*, IUCr Monographs on Crystallography, Oxford Science Publications, 1999.
46 P. Paoletti, R. Barbucci, A. Vacca and A. Dei, *J. Chem. Soc. A*, 1971, 310–313.
47 E. Elvingson, L. Baro and L. Petterson, *Inorg. Chem.*, 1996, **35**, 3388–3393.